

Thermoconductivity in Guest-Host Crystalline Systems.¹

E.I. Kats²

Laue-Langevin Institute, Grenoble, France

L.D.Landau Institute for Theoretical Physics RAS, Moscow, Russia

-
1. Not to be published in high impact factor journals.
 2. Collaboration with A.Muratov and H.Schober.

Thermoelectric devices are less pollutant as compared with conventional technologies. Unfortunately, poor efficiency inherent in the applications of thermoelectric materials.

- (i) During operation a material experiences a temperature gradient that must be maintained. Hence it is essential that its thermal conductivity be low.
- (ii) In contrast a material must have a high electrical conductivity (either to minimize energy dissipation, or to maximize the current).
- Serious problem, because (i) is usually characteristic of glasses, and (ii) is a characteristic of crystalline materials.
- Material must behave as phonon glass and electron crystal !
- Two ways to achieve it : either increase the electric conductivity of a glass, or reduce the thermal conductivity of a crystal.

What are Guest-Host systems ?

- Clathrate hydrates (water forms a crystal lattice of cages) ;
- Skutterudites or similar pyrochlor oxides (BCC compounds MT_4X_{12} , where M = alkali metal, alkaline earth, lanthanide or actinide, $T = Fe, Ru, Os$ and $X = P, As, Sb$ with structural polyhedral (distorted pentagon-dodecahedron) T_4X_{12} cages can be filled or unfilled by M) ;
- Group IV type I clathrates (simple cubic structure with 46 atoms per unit cell, X_{46} , where $X = Si, Ge, Sn$) ;
- Group IV type II clathrates (FCC structure with 136 atoms per unit cell, X_{136} , for empty cages, or $Na_{16}Cs_8Si_{136}$, where each of the 20-atom cages is occupied by guest Na and each of the larger 28-atom cages is occupied by Cs).

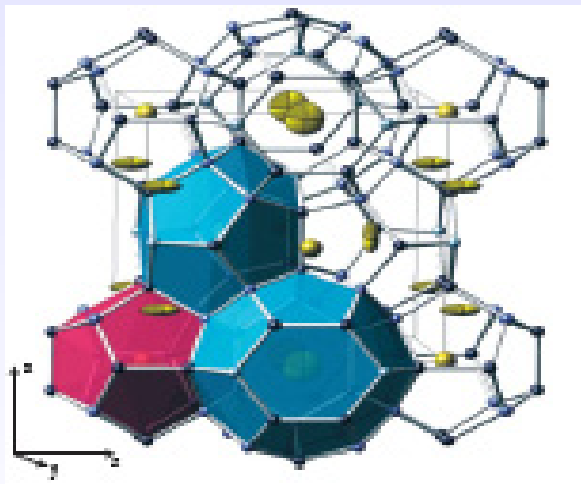


FIGURE: Typical guest-host structure

Contradictory observations to reconcile.

- Specific heats and thermal conductivities of clathrate compounds show almost identical thermal properties to those of glasses.
- However the disorder is less relevant as diffraction studies have provided the evidence that the structures of clathrate compounds are rather well defined.

What is known from numerical simulation side.

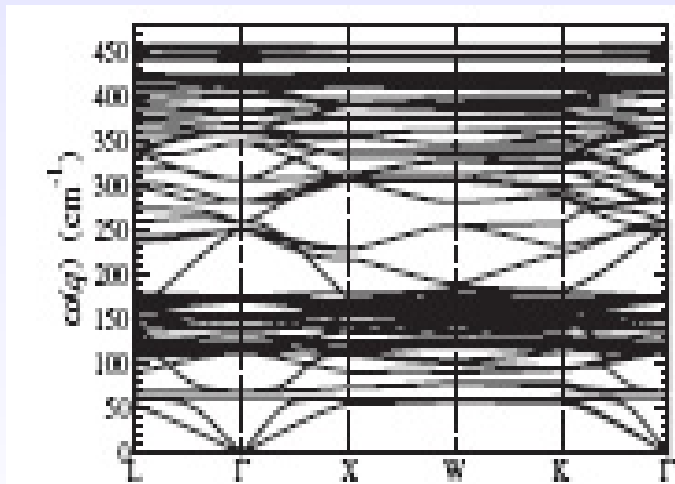
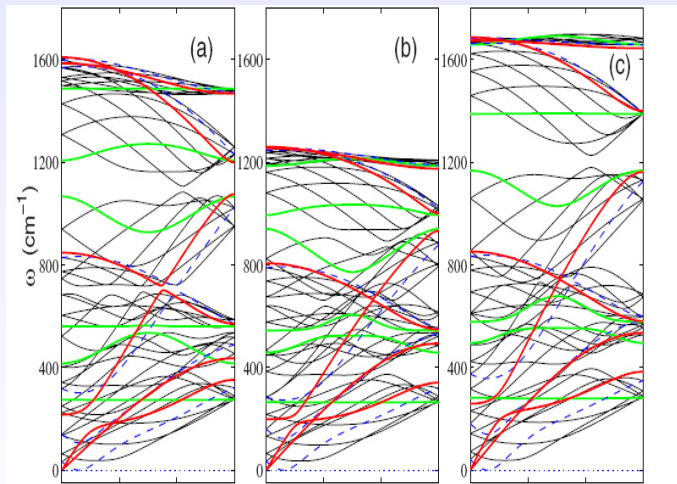


FIGURE: An example of numerically simulated dispersion laws.

One more example of numerical simulations



What is known experimentally. Thermoconductivity measurements.

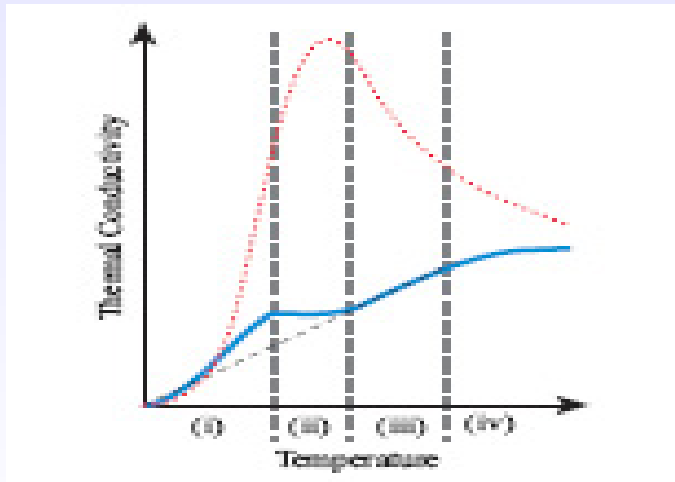


FIGURE: Thermoconductivity measurements. Solid line - experimental data in clathrates with off-centered guest ions ; dotted line crystalline like behavior ; dashed line linear T dependence.

To compare empty and filled cages.

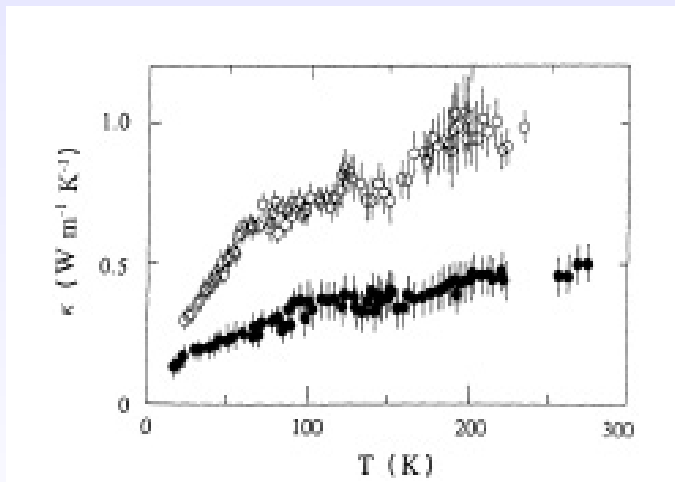


FIGURE: Thermoconductivity measurements : Upper curve -empty cages, lower curve - cages filled by off-centered guest ions.

To compare to glasses.

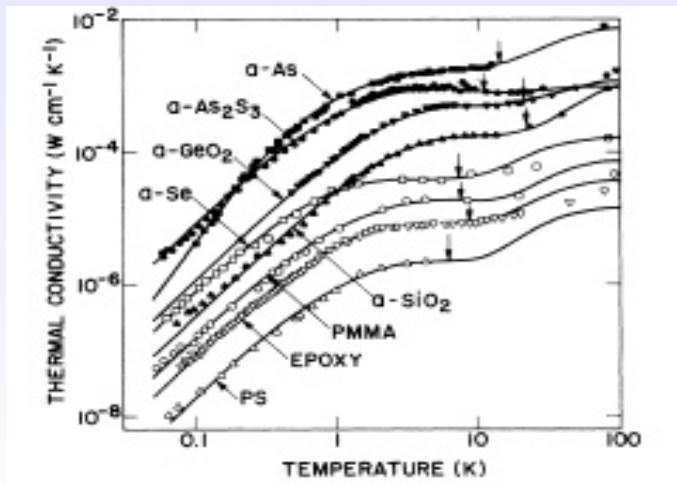


FIGURE: Thermoconductivity in glasses.

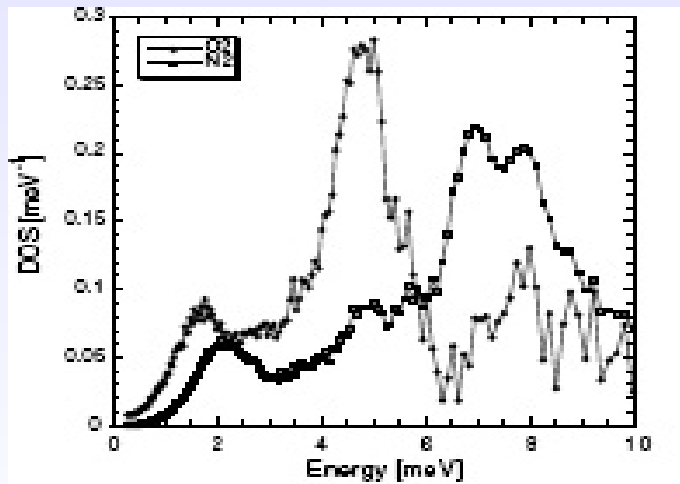


FIGURE: Data on density of states.

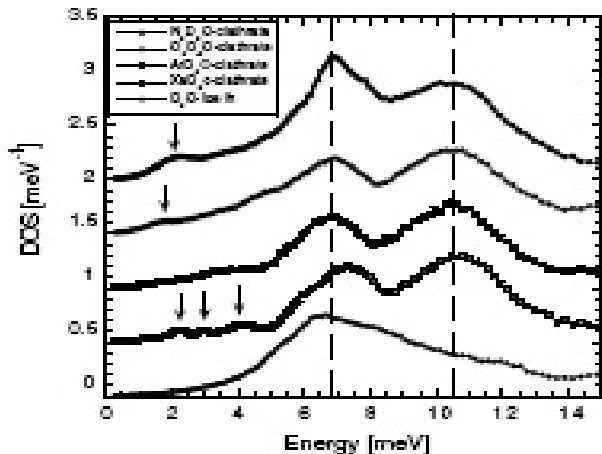


FIGURE: More experimental data on density of states

Einstein (rattler) oscillators versus soft optical modes.

- Observation of Einstein oscillators in solids is not unusual but they are normally observed in amorphous materials or in crystalline materials with impurities.

Cartoon guest-host model.

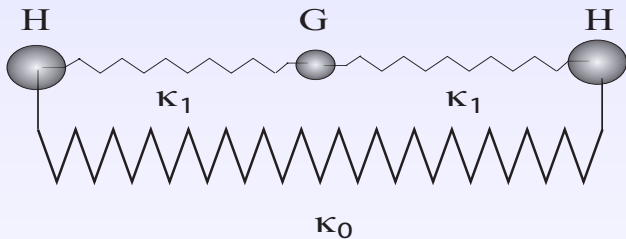


FIGURE: Springs are along a generalized coordinate for a soft mode

3D generalization of the model.

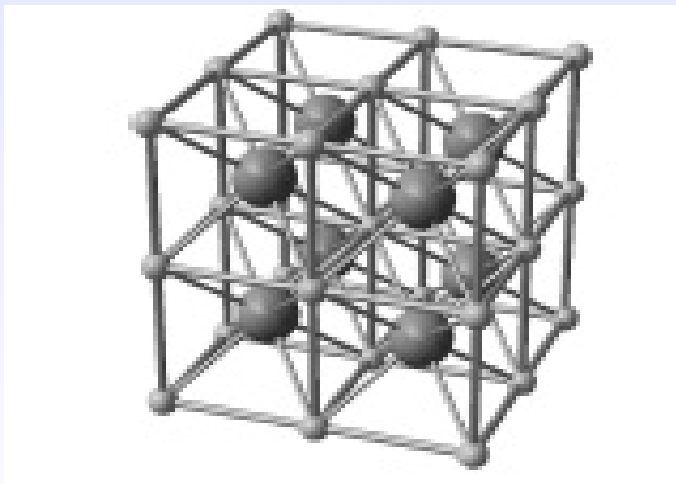


FIGURE: Simplest cubic guest-host structure.

Harmonic dispersion laws for cubic guest-host structure.

- Interaction potential

$$V = \sum_n \left(\frac{1}{2} \sum_{\delta} U_{hh}(|x_{h,n} - x_{h,n+\delta} - \delta|) + \sum_{\gamma} U_{gh}(|x_{h,n} - x_{g,n+\gamma} - \gamma|) \right)$$

where δ numerates 6 host neighbors, and δ - 8 guest neighbors.

- Atom equilibrium positions

$$3U'(d_{hh}) + 4\sqrt{3}U'(d_{gh}) = 0$$

with $d_{hh} = a$ and $d_{gh} = a\sqrt{3}/2$ being the equilibrium distances.

- From the 2-d order terms we derive dynamic matrix $\Phi_{\alpha\beta}^{ij}$ (α, β denote host or guest atoms, and i, j are Cartesian components for displacement vectors)

$$V_0 = \frac{1}{2} \sum_{k;ij;\alpha\beta} u_{-k,\alpha}^i \Phi_{\alpha\beta}^{ij} u_{k,\beta}^j$$

with

$$u_{k\beta} = \sqrt{\frac{m_\beta}{N}} \sum_n \exp(-ikR(n\beta)) x_{\beta;R(n\beta)}$$

where N is the number of unit cells and $u_{k\beta}^j$ is a displacement with respect to an equilibrium position $R(n\beta) = n + \delta_{\beta g} \mathbf{d}$.

Dynamic matrix.

- $$\Phi_{gg}^{ij}(k) = \delta_{ij}(\omega_g^2 + \Delta^2)$$
$$\Phi_{hh}^{ij} = \delta_{ij}[r(\omega_g^2 + \Delta^2) + (\omega_h^2 - r\Delta^2) \sin^2 k_i - r\Delta^2(\sin^2 k_i + \sin^2 k_j + \sin^2 k_m)]$$
$$\Phi_{gh}^{ij} = \sqrt{r} [-\delta_{ij}(\omega_g^2 + \Delta^2)\eta_k + (1 - \delta_{ij}\omega_g^2 \sin(k_i/2) \sin(k_j/2) \sin(k_l/2))]$$

where $r = m_g/m_h$, $\omega_g = (8U''_{gh}/3m_g)^{1/2}$, $\omega_h = 2(U''_{hh}/m_h)^{1/2}$, $\Delta = (8U'_{gh}/(m_g d_{gh}))^{1/2}$, and $\eta_k = \cos(k_x/2) \cos(k_y/2) \cos(k_z/2)$.

- For 2 atoms per unit cell, there are 6 modes some of which are degenerate in high symmetry points (e.g., in $\Gamma - R$ direction all branches are almost (over small parameter ω_g) degenerate).

Harmonic dispersion laws calculated for cubic guest-host structure.

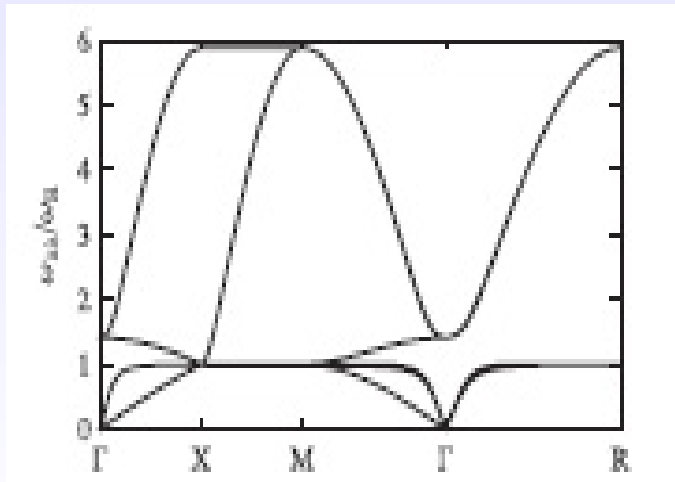


FIGURE: Phonon dispersion laws for the cubic guest-host structure : $\Gamma = (0, 0, 0)$, $M = (1, 1, 0)$, and $R = (1, 1, 1)$

Symmetric approximation : Dynamic matrix is taken as a scalar with respect to ij , independent of polarization



$$\Phi_{gg}(k) = \omega_g^2; \Phi_{gh} = -\sqrt{r}\omega_g^2\eta_k; \Phi_{hh} = \omega_{kh}^2 + r\omega_g^2$$

where $\omega_{kh} = \omega_h(\sin^2(k_x/2) \sin^2(k_y/2) \sin^2(k_z/2))^{1/2}$.

- The phonon spectrum

$$\omega_{\pm}^2 = \frac{1}{2}[(1+r)\omega_g^2 + \omega_{kh}^2] \pm \left(r\omega_g^4\eta_k^2 + \frac{1}{4}[(1-r)\omega_g^2 - \omega_{kh}^2]^2 \right)$$

Harmonic dispersion laws calculated in isotropic approximation.

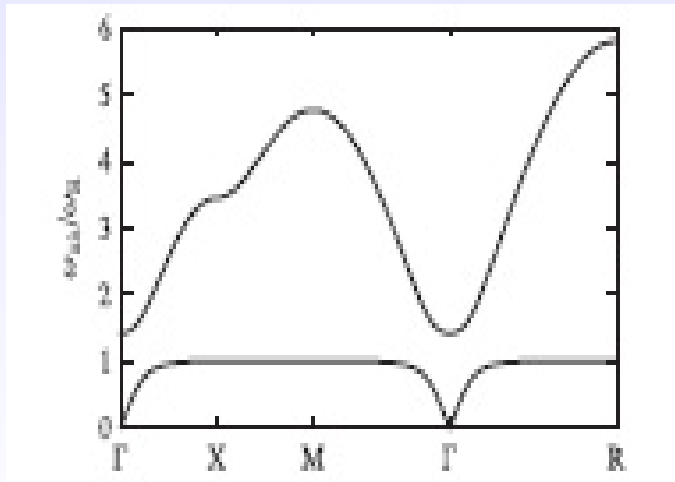


FIGURE: Phonon dispersion laws in isotropic approximation with $r = 1$, $\omega_h = 3.3$, and $\omega_g = 1$.

Anharmonic corrections.

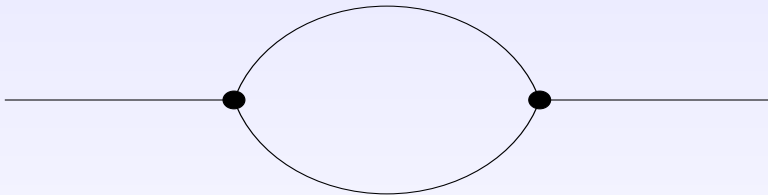


FIGURE: One loop diagrams describing phonon mode broadening.

Calculations.

- Hamiltonian in canonical phonon variables

$$H = \int \frac{d^3q}{(2\pi)^3} (\omega(q)a(q)a^*(q) + \int \frac{d^3p}{(2\pi)^3} \frac{V}{6} (a(q)a(p)a^*(q+p) + c.c.))$$

with the interaction vertex

$$V = \frac{qp(q+p)}{\sqrt{\omega\nu(\omega+\nu)}} \tilde{V}$$

- Inter-band coupling (decay of one optical or acoustic phonon into two acoustic phonons, or into one acoustic and one optic, and inverse coalescence processes, satisfying the selection rules, e.g., that created phonon must lie in a higher branch than at least of the destroyed phonons)

$$\gamma_1(\mathbf{q}) = \frac{\lambda q^2}{\omega_1(\mathbf{q})} \int_{-1}^{+1} dt \int_0^{\pi/2} p^2 f_1^2(p)$$

$$\left(\frac{f_1^2(\mathbf{s})(\gamma_1(\mathbf{p}) + \gamma_1(\mathbf{s}))(\omega_1(\mathbf{s}) - \omega_1(\mathbf{p}))}{(\omega_1(\mathbf{q}) + \omega_1(\mathbf{p}) - \omega_1(\mathbf{s}))^2 + (\gamma_1(\mathbf{p}) + \gamma_1(\mathbf{s}))^2} \right.$$

$$+ \frac{f_1^2(\mathbf{s})(\gamma_1(\mathbf{p}) + \gamma_1(\mathbf{s}))(\omega_1(\mathbf{s}) + \omega_1(\mathbf{p}))/2}{(\omega_1(\mathbf{q}) - \omega_1(\mathbf{p}) - \omega_1(\mathbf{s}))^2 + (\gamma_1(\mathbf{p}) + \gamma_1(\mathbf{s}))^2}$$

$$\left. + \frac{f_2^2(\mathbf{s})(\gamma_1(\mathbf{p}) + \gamma_2(\mathbf{s}))(\omega_2(\mathbf{s}) - \omega_1(\mathbf{p}))}{(\omega_1(\mathbf{q}) + \omega_1(\mathbf{p}) - \omega_2(\mathbf{s}))^2 + (\gamma_1(\mathbf{p}) + \gamma_2(\mathbf{s}))^2} \right)$$

where $\lambda = T \tilde{V}^2 / (2\pi)$, $f_{1,2}(\mathbf{p}) = |\mathbf{p}| / \omega_{1,2}(\mathbf{p})$, and $\mathbf{s} = |\mathbf{q} + \mathbf{p}|$.

Our results.

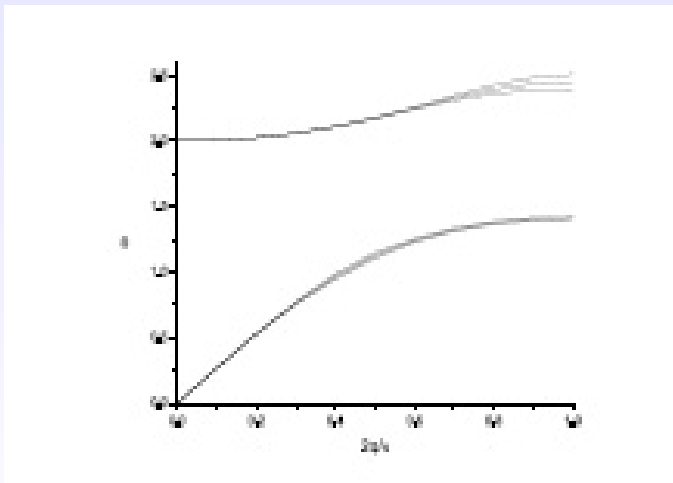


FIGURE: Spectrum and broadening for the force constants $k_0 \equiv 2(U''_{hh}/m_h)^{1/2} = 2$, $k_1 \equiv (8U''_{gh}/3m_g)^{1/2} = 2$.

Our results.

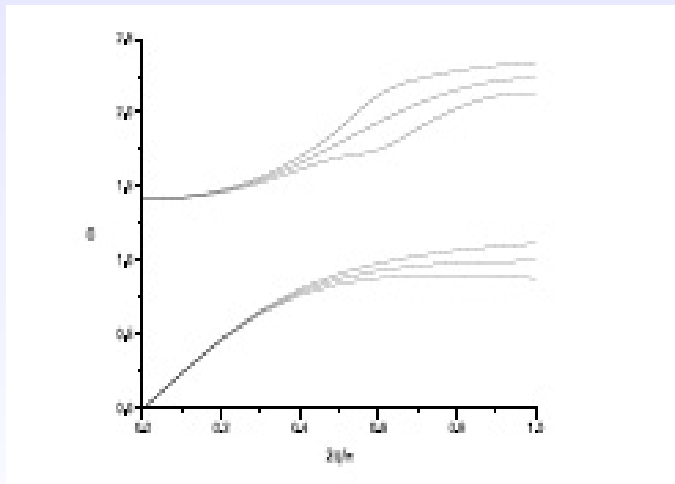


FIGURE: Spectrum and broadening for the force constants $k_0 = 2$, $k_1 = 1$.

Our results.

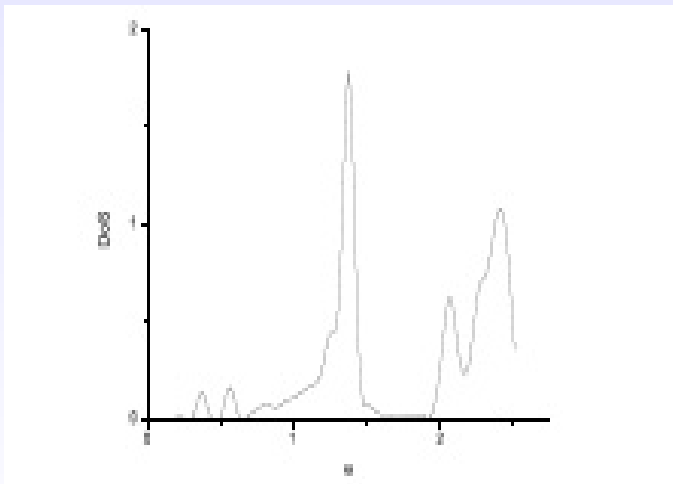


FIGURE: Density of states for the force constants $k_0 = 2$, $k_1 = 2$.

Our results.

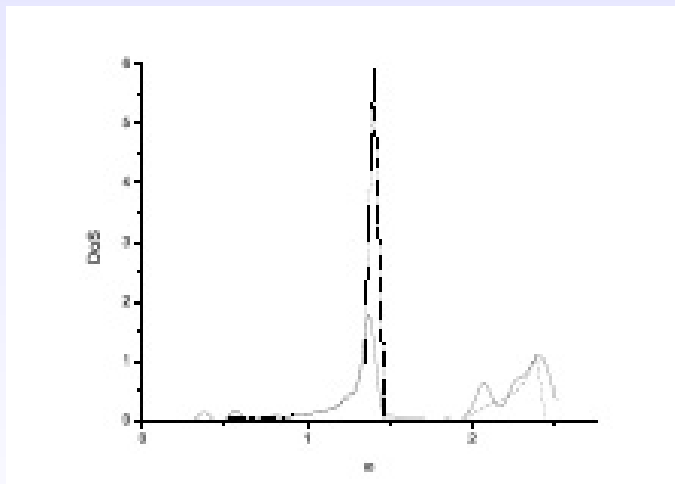


FIGURE: Harmonic density of states. Solid line shows anharmonic smearing of the singularities.

Our results.

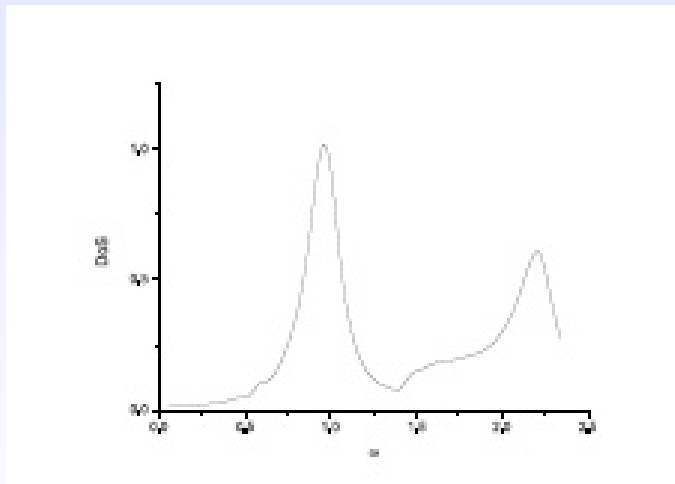


FIGURE: Density of states for the force constants $k_0 = 2$, $k_1 = 2$.

Our results.

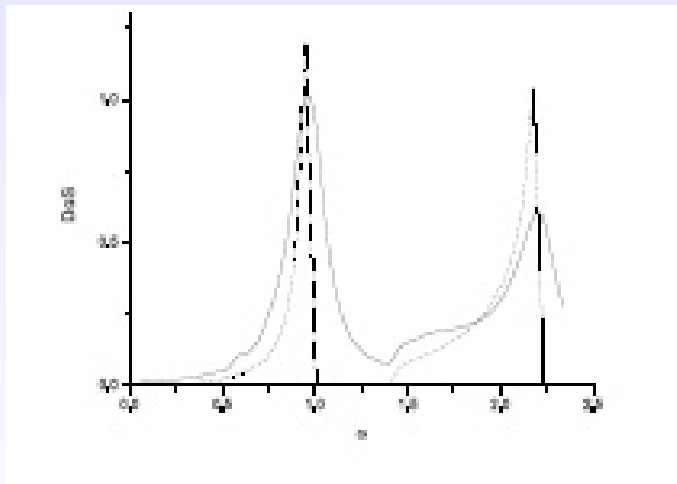


FIGURE: Harmonic density of states and anharmonic smearing.

Thermoconductivity

Thermal conductivity calculated from Boltzmann kinetic equation

$$\kappa = \sum_i \int dq q^2 \frac{C_i}{6\pi^2} \left(\frac{d\omega_i(q)}{dq} \right)^2 \frac{1}{\gamma_i(q)}$$

We find

$$\kappa(k_1 = 0.5k_0) \simeq 0.1\kappa(k_1 = k_0)$$

that is a relatively modest softening of the guest atom vibrations yields a noticeable reduction of thermoconductivity !

Not everything is so unclouded !

- κ is finite if three phonon mechanism of thermal conductivity is operational for all phonon branches (otherwise $\kappa = \infty$).
- The expression yields to a finite κ even if there were only normal (conserving quasi-momenta) processes, in contradiction to the notorious Peierls theorem.
- Luckily in our case (almost isotropic guest-host system) the predominant contributions into the integral do not come from small q (excluded by cut-off procedure).
- Normal collisions establish a local equilibrium and the Umklapp processes adapt this local equilibrium to the temperature gradient and establish a finite κ .

Where to go further on (1)

- Peierls-Boltzmann method is applicable to simple ordered crystalline materials. In such a case heat transport is realized by ballistically propagative (Bloch like) vibrational modes, scattered occasionally due to anharmonic effects, impurities, boundaries etc. At low temperatures, κ follows mainly specific heat temperature dependence, i.e., $\kappa \propto T^3$.
- At high temperatures propagating short wavelength phonons scattered by anharmonic interactions lead to $\kappa(T) \propto 1/T$.
- For disordered systems (like glasses) both T -dependence of κ and its magnitude are more or less material independent, whereas in crystals, κ values can be varied considerably.

Where to go further on (2)

- For sufficiently low temperatures, mean free path l for vibrational excitations (irrespective to system structural disorder) is relatively large (it is the principle distinction from electronic systems, there is no Anderson localization for phonons, even in so-called Ioffe-Regel limit, when $l \simeq a$, one may not define wave vector and Bloch-like wave functions, but phonons are still propagative excitations).
- For sufficiently low temperatures even in glasses one might apply Peierls-Boltzmann theory. However unlike crystalline materials, where l is so large that scattering mechanism is irrelevant, for disordered materials to explain T^2 low temperature behavior of $\kappa(T)$ one has to assume a special scattering mechanism (two level systems for instance) with $l \propto 1/T$.
- At the larger (intermediate) T in strongly disordered systems a sort of plateau for κ is observed and at higher temperatures $\kappa(T)$ increases with T , more or less linearly with a saturation at certain finite value $\kappa(\infty)$.

Where to go further on (3)

- Beyond the edge of the plateau the dominant vibrations propagate distances shorter than the hypothetical wavelength $2\pi v/\omega$. Thus, notions of wavelength or velocity cannot be assigned to these vibrations, but these higher frequency vibrations are not localized. The constant $\kappa(\infty) \neq 0$ indicates otherwise.
- Instead of ballistically transported heat one has to consider diffusive mode heat transport.

$$\kappa(T) \propto \sum_i D_i C\left(\frac{\hbar\omega_i}{2T}\right)$$

where C is the specific heat (for harmonic oscillator $C(x) = (x/\sinh x)^2$), and D_i is the mode i diffusivity.

- By simple dimensional analysis

$$D(\omega) = \frac{1}{3} a^2 \bar{\omega} f\left(\frac{\omega}{\bar{\omega}}\right)$$

where a and $\bar{\omega}$ are the characteristic length and frequency scales.

Where to go further on (4)

- Two simple choices for dimensionless function f (i) $f = c_1$, what means that a propagation (diffusion) length is of order a for all modes ; (ii)

$$f = c_2 \frac{\bar{\omega}}{\omega}$$

i.e., mode propagation length $\propto 1/\omega$.

- In a realistic guest-host system, its elementary cell includes about $N \simeq 50$ atoms, and this large number N is a very characteristic sign of disordered systems. In such a situation there are of order N narrow optical bands which repel each other making band widths and mode group velocities on average of order $1/N^{1/3}$. This geometrical fact replaces ballistic (Peierls-Boltzmann) heat transport by diffusive (glass-like) heat transport.

Last Speculations

- A bit symbolically

$$\kappa(T) = \sum_i \left[\int_0^{\omega_0} C_i(\omega) v_i^2(\omega) \tau_i(\omega) d\omega + \int_{\omega_0}^{\omega_D} C_i(\omega) D_i(\omega) \right]$$

where the 1-st contribution comes from Peierls-Boltzmann ballistic transport and the 2-d term occurs due to diffusive optical modes. ω_0 is a characteristic frequency separating the both regimes.

- For diffusive transport : low temperature T^2 , saturation at finite constant value $\kappa(\infty)$ at high temperatures. If ballistic transport dominates the thermoconductivity, κ follows T^3 law at low temperatures and $1/T$ law at high temperatures.

To confront theory and thermoconductivity measurements.

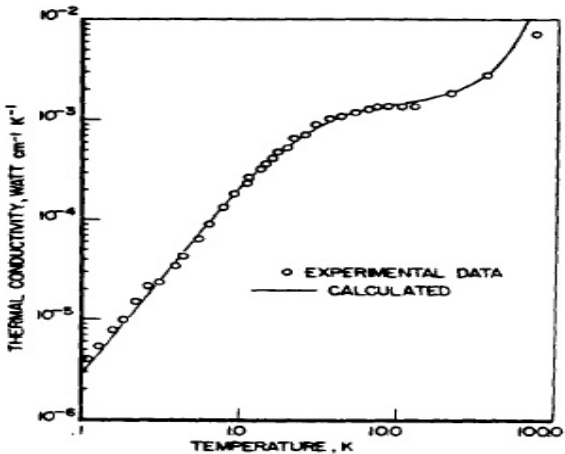


FIGURE: Thermoconductivity measurements for tetrahydrofuran THF – 17 H₂O.

Typical numbers

- Minimal $\kappa \propto 2.7 \text{ Wm}^{-1} \text{ K}^{-1}$ (room temperature).
- For crystalline *Ge* $\kappa \propto 114 \text{ Wm}^{-1} \text{ K}^{-1}$.
- For amorphous *Ge* $\kappa \propto 0.62 \text{ Wm}^{-1} \text{ K}^{-1}$.
- $S \simeq 10^2 \mu\text{eV}/\text{K}$,
- "figure-of-merit" $Z = S^2 \sigma / \kappa$ for the best thermoelectric material Bi_2Te_3 , $ZT \simeq 1$ (at $T = 300 \text{ K}$), for a typical filled skutterudite, $ZT \simeq 1.6$.